Engineering Applications of Artificial Intelligence 105 (2021) 104405

Contents lists available at ScienceDirect

Engineering Applications of Artificial Intelligence

journal homepage: www.elsevier.com/locate/engappai

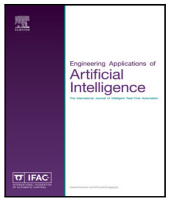

# Assessment of the running resistance of a diesel passenger train using evolutionary bilevel algorithms and operational data

Luciano Sánchez [a,*], Pablo Luque [b], Daniel Álvarez [b]

[a] Departamento de Informática, Universidad de Oviedo, Spain
[b] Departamento de Construcción e Ingeniería de Fabricación, Universidad de Oviedo, Spain

ARTICLE INFO

*Keywords:*
Railways
Passenger trains
Evolutionary algorithms

ABSTRACT

Evolutionary bilevel algorithms are used for approximating the running resistance on the basis of the long-term fuel consumption data of a diesel passenger train in different routes. The input data comprises the geometry of these routes, speed and acceleration limits and certain engine properties. A running resistance is found for which the consumptions predicted by the model are equal to the logged consumptions of the vehicle for each of the routes in the training set. The model has been validated with simulated data with known properties and also with a diesel-hydraulic railcar operating on a 94 km route in northern Spain. The error in the running resistance estimation using evolutionary algorithms with respect to the measurement with a coasting test was less than 4%.

## 1. Introduction

Following the European Parliament's directive 2014/94 on the deployment of alternative fuels infrastructure, traction tests of a Liquified Natural Gas (LNG) powered passenger train were carried in the north of Spain in the second semester of 2019. The engine of a Diesel-hydraulic Multiple Unit (DHMU) of the RENFE S2600 Series (see Fig. 1) was replaced by an LNG engine and a large set of compared measurements was collected. The purpose of this study was to assess the improvements in fuel costs and emissions if the Spanish fleet of diesel passenger trains was transformed to LNG.

Diesel engines in S2600 vehicles complied with a directive that is no longer in force (EURO II) but the tested LNG engines fulfil the regulations current in 2020. A substantial reduction in pollutants is therefore expected, mainly in nitrogen oxides and particulate matter (Suarez-Bertoa et al., 2020). Notwithstanding this, the aforementioned tests have shown that improvements in carbon monoxide (CO) and greenhouse emissions heavily depend on the engine operating point. Because of this, the extrapolation of the test results is not immediate: the environmental impact of transforming a fleet of diesel passenger trains to LNG depends on the characteristics of chosen routes, such as their horizontal and vertical geometry or the number of stops (Pan et al., 2019).

Predictive models are a cost-effective method for assessing the environmental impact of the transformation to LNG, not requiring the measurement of emissions along the different routes. Many of the existing models are based on a good correlation between the engine emissions and the operating point, which is defined by the pair torque–engine speed and other variables of secondary importance (Yu et al., 2020). The operating point, in turn, can be directly measured in the vehicle or be approximated by a model of the longitudinal dynamics that takes into account longitudinal speed, mass and running resistance (Wang and Rakha, 2018). Mechanical losses in the power train (transmission, mechanical losses, auxiliary consumption, etc.) are also included in these models (Tormos et al., 2020).

Arguably, the input variable that is hardest to obtain is the running resistance. Standard procedures for measuring the running resistance include coasting tests in railway lines (Somaschini et al., 2016). These measurements, when possible, are expensive. Alternatively, there are machine learning-based procedures that allow the running resistance to be obtained from operational data. For instance, it has been demonstrated (Hansen et al., 2017) that a time-series of energy consumption and velocity values, taken from the Vehicle Control Unit (VCU), suffices to determine the resistance to motion of trains, without knowing the characteristics of the track.

From a formal point of view, obtaining the running resistance of a train by means of intelligent techniques is an inverse problem, which consists of recovering the parameters of a physical system (or "forward model") that has produced a set of measurements (Tarantola, 2005). In most applications of AI to inverse problems, an optimisation algorithm is used to obtain some of the inputs of the forward model given the remaining inputs and the output. The forward model, in turn, can also be obtained by machine learning (Nino-Ruiz, 2021).

* Corresponding author.
*E-mail address:* luciano@uniovi.es (L. Sánchez).

https://doi.org/10.1016/j.engappai.2021.104405
Received 22 October 2020; Received in revised form 7 June 2021; Accepted 25 July 2021
Available online 9 August 2021


**Fig. 1.** LNG-propelled paired automotive unit, RENFE Series 2600.
*Source:* RENFE Sala de Prensa.

In the case at hand, the forward model concerns the prediction of the vehicle energy consumption. The running resistance is one of the unknown inputs. According to Martínez Fernández et al. (2019), the modelling methods for railways energy consumption are mostly based on the Davis equation (Davis, 1926), because terms can be added to this equation relating energy consumption to traction effort, resulting in a modular model whose complexity can be increased by terms such as ancillary consumption or driver behaviour. Other authors opt for simplified energy models (Su et al., 2018) that can be embedded in real-time controllers or, at the other end of the spectrum, neural networks (Pineda-Jaramillo et al., 2020), which can describe complex dynamic behaviours but require representative datasets, which are not always available. The most frequently used optimisation algorithms are Tabu Search (Huang et al., 2017), Evolutionary Algorithms (ShangGuan et al., 2015), Ant Colony (Eaton et al., 2017), Particle Swarm (Yang et al., 2015) and Teaching Learning Based Optimisation (Huang et al., 2015).

Depending on the intended application, the inputs to the forward model may include additional variables to the minimum set (i.e. speed profile, slope and track curvature). For example, reinforcement learning was used in Tang et al. (2020) to optimise a model that included the properties of the traction and braking subsystems as inputs. Finally, the speed profile, which in turn depends on driving constraints and driver's actions, can also be optimised. In Sicre et al. (2014) Genetic Algorithms were deployed to optimise a profile that depended on a fuzzy characterisation of train drivers' behaviour. In Fernández-Rodríguez et al. (2020) a Multi-Objective Particle Swarm optimisation of the speed profile was introduced. Lastly, in He et al. (2021) Differential Evolution was applied to search for the speed profile with the lowest energy consumption, taking into account the passenger flow at the stations.

With the same objective as Hansen et al. (2017) in mind, the main contribution of this study is a new method for approximating the running resistance from operating data. We suggest that the long-term average fuel consumption data of a diesel train on different routes, obtained from the refuelling logs, contain enough information to estimate the running resistance. The accuracy of the estimation depends on the error margin of the fuel measurements, but in practical circumstances it will be enough for making a reasonable prediction of the consumption and emissions of the transformed LNG vehicle on the same routes. Contrary to previous models that use operating data, the present study does not employ dedicated sensors, nor does it access the VCU, the input data being limited to:

1. Average fuel consumption of the diesel vehicle on a set of routes.
2. Horizontal and vertical geometry of the routes.
3. Speed limits.
4. Accelerations (and braking) limits.
5. Brake-Specific Fuel Consumption (BSFC) and maximum torque of the engines.

An inverse problem is solved in which the unknown variables are the velocity profile and the running resistance. The forward model is based on an augmented version of the Davis equation that includes properties of the traction and braking subsystems, the route layout and the slopes of the track sections. The proposed solution makes use of an evolutionary bilevel optimisation algorithm (Sinha et al., 2020) where one optimisation method is used within the other (see Section 2). The outer algorithm finds an expression of the running resistance for which the predicted fuel consumption along the chosen set of routes matches the measured average consumption. The inner algorithm finds a plausible velocity profile for each of the routes (profiles fulfilling speed, acceleration and diesel engine torque limits). This nested structure is needed because the prediction of the fuel consumption depends on the velocity profile, and the velocity profile depends in turn on the unknown running resistance. It will be shown in Section 3 that the forward model and the velocity profile can be accurately recovered from the average consumptions on a reduced set of routes. Experiments with a real DHMU are provided in the same section, confirming that the results of the proposed procedure are consistent with coasting tests.

## 2. Proposed method

The method presented here searches for an expression of the running resistance that minimises the difference between the measured fuel consumption and its model-based prediction in a "training set" comprising different routes.

### 2.1. Forward model: fuel consumption of a DHMU

The solution of inverse problems with Artificial Intelligence techniques boils down, as mentioned in the introduction, to the application of an optimisation algorithm to the prediction of the inputs of the direct model, given its outputs. Since each evaluation of the objective function requires evaluating the fuel consumption model along several routes, it

is necessary to search for a model that is computationally simple and yet sufficiently accurate, relying on several simplifications.

The energy required to move the vehicle depends on its mass, the speed profile, the running resistance and the mechanical resistances in the drive system. These factors are not independent of each other and are influenced by exogenous variables. The mass depends on fuel consumption and the number of passengers. The speed profile depends on the driver's actions, the control system, passenger access at stops, unexpected delays and the engine nominal power (Martínez Fernández et al., 2019). Rolling resistance depends on aerodynamic factors, track layout (curves, tunnels), mechanical resistances (starts and stops), etc.

The relationship between the heat output of the fuel consumed in the engine and the power delivered to the wheels depends on the engine characteristics and the mechanical efficiency of the transmission. On the one hand, the thermodynamic efficiency of the engine depends on its operating point; in steady state, this dependence is expressed by the BSFC curves mentioned above. On the other hand, the mechanical inefficiencies of the different parts of the transmission can be grouped into a factor $\eta$ which relates the power generated by the engine to the power delivered to the wheels of the vehicle. This performance is not constant. For example, in the DHMU studied in this work, the gearbox has two modes, hydraulic and mechanical, with different efficiencies. The gearbox automatically shifts from one mode to another depending on the vehicle speed and, therefore, efficiency changes abruptly when a certain speed is reached.

The model used in this study is based on the following simplifications:

1. Transmission efficiency depends only on speed.
2. The instantaneous fuel consumption of the engine depends only on the torque and speed.
3. Mass changes due to passengers boarding and alighting are weighted along the entire circuit.
4. The speed profile is the one that allows completing the route in the minimum possible time, given the maximum acceleration and braking restrictions allowed in a passenger vehicle and the engine torque curves.

The latter simplification is debatable, because it neglects the effect of the driver on fuel consumption. During manual driving of the vehicle, there are indications on the track as to the speed to be reached or the point at which to initiate braking. According to the experiments described in Martinez-Garcia and Gordon (2018) and Martinez-Garcia et al. (2019), drivers react to visual stimuli after a certain time delay. Some of these experiments have been performed with a joystick similar to the one used to control the railcar, so it is reasonable to assume that such variability in reaction times will introduce uncertainty in the model output. In high-speed trains, the effect of driving on energy consumption has been simulated in Sicre et al. (2014) for a driving strategy consisting of keeping the vehicle at the nominal speed for as long as possible, accelerating and decelerating in well-defined positions.

Taking these studies into account, the above four simplifications have been applied in the proposed model. However, to assess their importance in the predictions of our model, we have also performed a series of simulations in Section 3.2.1 in which random changes in acceleration and deceleration positions are introduced, compensating the differences in travel time with increases and decreases in stopping times.

### 2.2. Route discretisation

Each of the considered routes is divided into a list of $N$ segments, correlative and short enough to allow the acceleration on each of them to be regarded as constant (thus the vehicle speed changes linearly in the segment) and both the slope and the track curvature are also constants (Peralta et al., 2018). Formally, segments are tuples $(s_i, \sigma_i, a_i, c_i, v_i)$, with $i = 1 \dots, N$, where $s_i$ is the segment length, $\sigma_i$ is the slope, $a_i$ is the acceleration, $c_i$ is the curvature and $v_i$ the longitudinal speed at the beginning of the segment. We will call the position of the vehicle on the path $x$, $0 \le x \le s_1 + \cdots + s_i$, and $x_i$ is the distance between the origin of the $i$th segment and the starting point of the test circuit,

$$x_i = \begin{cases} 0 & i = 1 \\ x_{i-1} + s_{i+1} & \text{otherwise.} \end{cases} \tag{1}$$

The vehicle mass is $m$. The time elapsed from when the vehicle starts moving is $t$, and the time used to reach the beginning of the $i$th segment is $t_i$, thus

$$v(t) = \left.\frac{dx}{dt}\right|_{x(t)} \tag{2}$$

with $v_i = v(t_i)$.

### 2.3. Vehicle simulation: torque and fuel consumption

The tractive effort $te_i$ at the starting point of the $i$th segment is defined as Wu et al. (2016)

$$te_i = (1+\epsilon)m \cdot \frac{d^2x}{dt^2}(x_i) + m \cdot g \sin(\sigma_i) + \mathrm{R}(v_i) + \mathrm{R}_c(c_i) \tag{3}$$

where $\epsilon$ compensates the inertia of the rolling elements in the powertrain, R is the train resistance force as a function of the velocity (Rochard and Schmid, 2000) and $\mathrm{R}_c$ is the resistance due to curvature. In this study, the Davis' quadratic expression is used

$$\mathrm{R}(v) = A \cdot v^2 + B \cdot v + C \tag{4}$$

and tunnels are not considered.

Let $n_m$ be the number of engines and $p_i^{aux}$ the power demanded by the auxiliary elements on the $i$th segment. Two assumptions are introduced in the model that simplify the calculations with a minor impact on the accuracy of the model: (a) all engines in the unit rotate at the same speed $\omega_i$ and (b) the mechanical efficiency of the powertrain is a function of the longitudinal velocity,

$$\eta_i = \eta(v_i). \tag{5}$$

S2600 units have a hydrodynamic-mechanical transmission. When in mechanical mode, the rotational speed depends on the longitudinal velocity. At lower speeds it will be assumed that the capacity of the torque converter is high enough to consider that the engine speed is independent of the train speed and an energy balance can be calculated for each segment. That is to say, for transmissions in mechanical mode the engine speed depends on the longitudinal speed

$$\omega_i = \omega(v_i), \tag{6}$$

thus the engine torque is

$$T_i = \begin{cases} \left(te_i \cdot v_i \cdot \eta_i^{-1} + p_i^{aux}\right) / (n_m \cdot \omega(v_i)) & \text{if } te_i > 0 \text{ (tractioning engine)} \\ p_i^{aux} / (n_m \cdot \omega(v_i)) & \text{if } te_i \le 0 \text{ (braking or stopped vehicle),} \end{cases} \tag{7}$$

and when in hydraulic mode, the engine rotates at its nominal speed $\omega(v_i) = \omega_0$. Lastly, we will assume that the instantaneous fuel consumption depends on the torque and the rotational speed through a function BSFC (Brake-Specific Fuel Consumption) that returns the fuel consumption in grams per second, thus the fuel consumption on the $i$th segment is

$$\mathrm{fuel}_i = \frac{1}{2}(\mathrm{BSFC}(T_i, w_i) + \mathrm{BSFC}(T_{i+1}, w_{i+1})) \cdot (t_{i+1} - t_i) \tag{8}$$

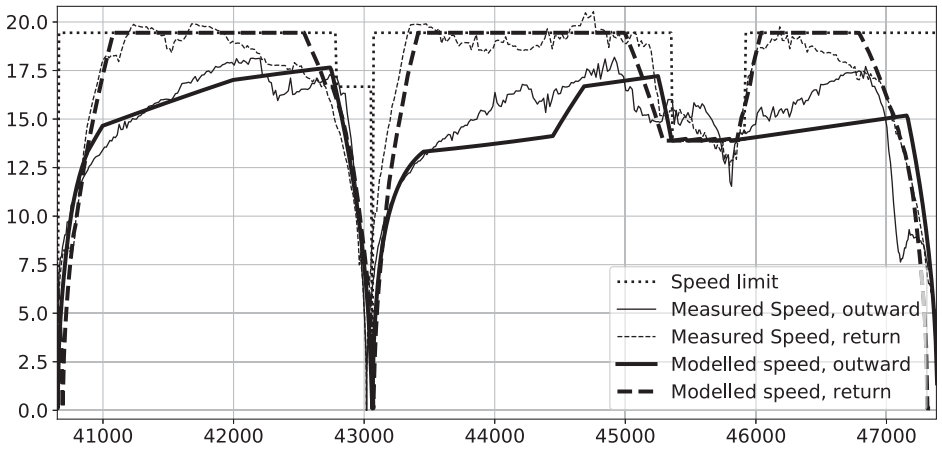


**Fig. 2.** Actual (GPS-measured) velocity (m/s) and computer-generated profile for an S2600 unit, on the Trubia-Collanzo route (Asturias, Spain). Kikuchi's algorithm produces the dotted line in both directions, but the engine is not powerful enough to reach the commercial speed in part of the outward route (solid curves), where there are gradients as high as 16 ‰. The proposed method is able to find a reasonable approximation through a model that makes use of the characteristics of the engine, the transmission and a rough approximation of the grades on the route. It is important to note that the measured speed is only used for validation purposes and was not used in the calculations to obtain the computer-generated profiles.

### 2.4. Inner problem: Approximated velocity profiles

Let $v(x)$ be the unknown speed profile, $I$ the set of indices of the segments that contain stops and let $t_i^{stop}$, $i \in I$ be the stopping times. The time needed for reaching the destination (the end point of the $N$th segment) is

$$t_{N+1} = \int_0^{x_N+s_N} \frac{1}{v(x)} dx + \sum_{i\in I} t_i^{stop}. \tag{9}$$

If the actual speeds on the route were known, it would make sense to minimise the difference between Eq. (9) and field data. For instance, in Besinovic et al. (2013) this problem was solved with genetic algorithms on the basis of a longitudinal dynamic model and a route discretisation similar to that used in this paper. In this paper it is not assumed that field data is available, thus a different approach must be followed. As mentioned in the introduction, a bilevel optimisation algorithm is deployed to find the combination of profile and resistance that matches the measured consumptions on the training routes. In the remainder of this subsection the inner problem, which is estimating the velocity profile given the running resistance, is explained.

Let the speeds at the starting points of each segment be $v_i = v(x_i)$ and let $\tau_i = t_{i+1} - t_i$. The purpose of the presented algorithm is to determine the set of values $v_i$ that best fulfil a certain set of conditions. Given that the acceleration on the $i$th segment was assumed to be constant, the time elapsed on the $i$th segment is obtained by solving the equation

$$s_i = v_i \cdot \tau_i + a_i \frac{\tau_i^2}{2} \tag{10}$$

and

$$a_i = \frac{v_{i+1} - v_i}{\tau_i}. \tag{11}$$

Let

$$v_i^{\text{avg}} = \frac{1}{2}(v_{i+1} + v_i) = \frac{1}{2}(v_i + \sqrt{v_i^2 + 2as_i}). \tag{12}$$

The time elapsed on the whole route is

$$t_{N+1} - \sum_{i\in I} t_i^{stop} = \sum_{i=1}^{N} \frac{2s_i}{v_{i+1} + v_i} = \sum_{i=1}^{N} \frac{s_i}{v_i^{\text{avg}}}. \tag{13}$$

There are recent procedures for obtaining the velocity profiles of a train that combine the running resistance and a driving model (Sicre et al., 2014). In this study the engine power is a limiting factor and furthermore a fast algorithm is needed that can be called from the fitness function of a metaheuristic, thus it is proposed that the values $v_i$ are found by means of a modified Kikuchi's algorithm (Kikuchi, 1991), subjected to the following three constraints:

1. Let $a^-$ and $a^+$ the maximum deceleration and acceleration values. Let $v(t) = v(x(t))$. If $v(t) > 0$, then

$$\frac{dv(x)}{dx} = \frac{dv(x(t))}{dt}\frac{dt}{dx(t)} = \frac{dv(t)}{dt}\frac{1}{v(t)}, \tag{14}$$

and the velocity profile must fulfil the requirement that

$$a^- \le \frac{dv(t)}{dt} = v(x)\frac{dv(x)}{dx} \le a^+, \tag{15}$$

which is discretised as follows:

$$a^- \le v_i^{\text{avg}} \cdot \frac{v_{i+1} - v_i}{s_i} = \frac{v_{i+1}^2 - v_i^2}{2s_i} \le a^+. \tag{16}$$

2. Velocities are always positive and subject to the following limits:

$$v_i \in [0, v_i^{max}] \quad \text{for } i \text{ in } \{1 \dots, N\}, i \notin I. \tag{17}$$

Let also the designated stops be placed at the beginning of their corresponding segments, thus

$$v_i = 0 \quad \text{for } i \text{ in } I. \tag{18}$$

3. There are routes where the engine torque is not enough to attain the required acceleration (see Fig. 2). The torque limit cannot be entered in the Kikuchi's algorithm as a limit on acceleration or speed, because the feasible speed depends on the simulated torque values, which depend in turn on the running resistance. We propose that the acceleration $a_i = a(x_i)$ is reduced for every segment where the torque limit is violated, until the resulting velocity profile can be accomplished for the tested running resistance.

In the presented implementation, the reduced acceleration values $a_i$ are obtained by Sequential Quadratic Programming (Boggs and Tolle, 1995). The following constrained optimisation problem is solved for

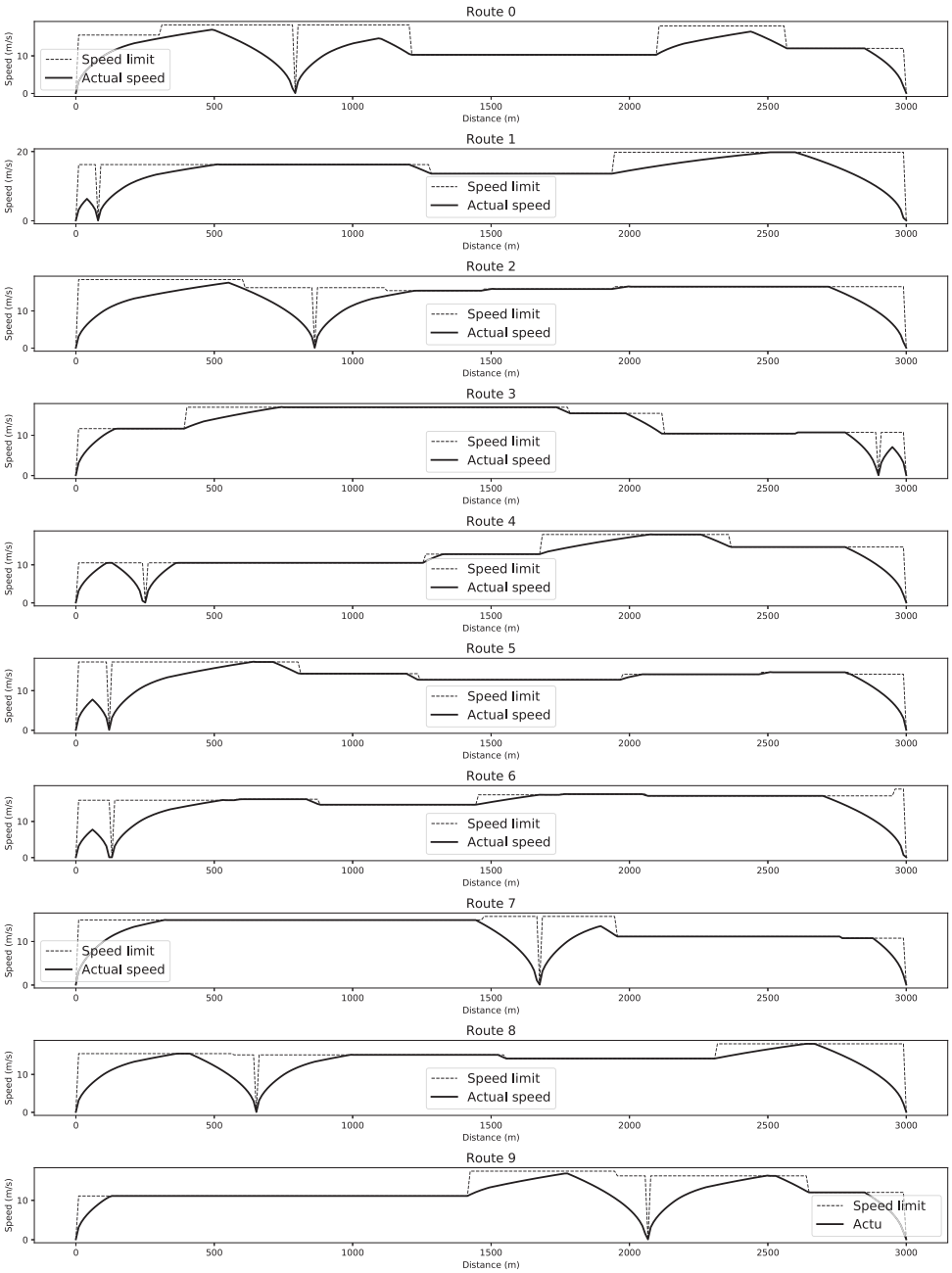


**Fig. 3.** Training routes. All routes are 3000 m long and the maximum speed is 15 m/s. Each route has a single stop. The maximum gradient (not shown) is 6 ‰. Acceleration and deceleration are limited to 0.5 m/s$^2$.

each of the segments:

$$
\begin{aligned}
&\textbf{maximize} a_i \\
&\text{subjected to:} \\
&(n_m \cdot T_i \cdot \omega(v_i^{\text{avg}}) - p_i^{aux}) \cdot \eta_i - m \cdot v_i \cdot (g \sin(\sigma_i) + \mathrm{R}(v_i^{\text{avg}}) + \mathrm{R}_c(c_i)) \geq (1+\epsilon) m \cdot a_i \\
&T_{\max}(\omega(v_i^{\text{avg}})) \geq T_i \\
&a_i \geq a^- \\
&a^+ \geq a_i.
\end{aligned}
\tag{19}
$$

and defining

$$
v_i = \begin{cases} v_{i-1} + \sqrt{v_{i-1}^2 + 2 a_i s_i} & \text{if } i > 1 \text{ and } i \notin I \\ 0 & \text{if } i = 0 \text{ or } i \in I. \end{cases}
\tag{20}
$$

In Fig. 2 actual (GPS-measured) velocity and a computer-generated profile for an S2600 unit, on the Trubia-Collanzo route (Asturias, Spain) are shown. The differences between the commercial speed (dotted line), Kikuchi's approximation (dashed line) and the proposed method (solid line) are significant on the outward path. Observe that a reasonable approximation to the engine operating points is possible, given a rough measurement of the grades at each point on the route, without using GPS sensors, nor accessing the VCU.

### 2.5. Definition of the outer problem: fuel consumption

If the running resistance $R$ is known, the problems defined in Eq. (19) are solvable for all $i$. Torque $T_i$, engine speed $w_i$ and time $t_i$ can be obtained for each segment. Recalling Eq. (8), the consumption

along a route can be estimated as

$$\text{fuel}(R) = \sum_{i=1}^{N} \text{fuel}_i. \tag{21}$$

Given this relationship between the running resistance and the fuel consumption, it also makes sense to solve the inverse problem: given a set of consumptions in different routes and the model defined in the preceding section, find the most plausible expression for $R$.

Let us suppose that there are $k$ routes whose predicted consumptions are $\text{fuel}_r(R)$ with $r = 1, \dots, k$. These are functions of the unknown running resistance $R$ and the properties of the route (commercial speed, gradients, etc.). Let the measured average consumption on the $r$th route be $c_r$. If the running resistance is defined by the Davis equation,

$$R(v_i) = A + B \cdot v_i + C \cdot v_i^2 \tag{22}$$

then an approximation to $R$, in a least squares setting, is

$$(A, B, C) = \arg\min_{\mathbf{x}\in\mathbb{R}^3} \sum_{r=1}^{k} (c_r - \text{fuel}_r(\mathbf{x}))^2. \tag{23}$$

It should be said that evaluating the fuel consumption along a route for a given running resistance requires solving as many quadratic problems as there are segments in the route (recall Eq. (19)), thus solving Eq. (23) will be computationally hard. In the following subsection we discuss the application of a recent metaheuristic that is able to solve this bilevel problem in an efficient manner.

### 2.6. Metaheuristics for solving bi-level problems

It is well known that solving quadratic bilevel problems by descent algorithms can be an NP-hard problem (Vicente et al., 1994). We have found that solving $N$ inner quadratic problems (see Eq. (19)) for every evaluation of $\text{fuel}_r$ when solving Eq. (23) by descent algorithms is unfeasible except in small datasets. The problem is bad conditioned, with many local minima, and descent algorithms are heavily dependent on the starting point.

Evolutionary algorithms are less influenced by the presence of multiple local minima, but the computational cost is much higher. There are, however, recent studies in evolutionary bilevel problems, such as that of Sinha et al. (2020), that exploit the mathematical properties of the inner problems and are able to perform approximations that speed up the calculations. In this study, the BLEAQ-II algorithm (Bilevel Evolutionary Algorithm based on Quadratic Approximations) will be adapted to the problem being studied. In our case, a map of the inner problem will be built that exploits the similarities between the velocity profiles of analogous running resistances. When a running resistance that is similar to a previously evaluated candidate is found, the velocity profile will not be obtained by solving the quadratic optimisation problem, but it will be interpolated from the nearest individuals in the archive, with significant computational savings. The proposed application of BLEAQ-II is as follows:

1. **Initialization**: An initial population of running resistances of size $P$ is generated at random. The inner level problem is solved for each of these individuals. All individuals are tagged with the value **1**. A copy of each individual, velocity profile and fitness is kept in an archive.
2. **Reproduction**: $2\mu$ individuals are selected from the population and a tournament selection is performed to obtain $\mu$ parents. $\lambda$ offspring are generated using genetic operators.
3. **Offspring Update**: For each of the offspring running resistances generated in the previous step, the corresponding velocity profile is computed following one of the following strategies:
   (a) If the number of individuals in the population with tag **1** is less than a limit $Q$, the inner problem is solved and the new individual receives the tag **1**. The new individual is added to the archive.
   (b) If there are at least $Q$ individuals tagged **1** in the population, the velocity profile of the new individual is interpolated from the neighbour members in the archive. The three individuals in the population that are nearest to the offspring running resistance are selected, and quadratic interpolation is used for estimating the speed for all the segments of the training routes. If the distance between the individual being evaluated and the nearest neighbour is low, then the inner problem is solved and the resulting fitness value is assigned to the individual, which is tagged with the value **0**. Interpolated individuals are not added to the archive. If the distance to the nearest individual in the archive is high, or the resulting fitness becomes the elite of the current population, the true velocity profile of the individual is recomputed by solving Eq. (19), fitness and tag are updated and the individual is added to the archive.

   Once the velocity profiles are computed, $\rho$ members of the population are selected at random and sorted by tag (first) and by fitness, and the worst $\lambda$ of them are replaced by the offspring.
4. Go to Step 2 or end if the termination conditions are met.

Parent Centric (PCX) crossover and polynomial mutation were used as genetic operators, with the same definition and parameters shown in Sinha et al. (2020).

**Table 1**
Parameters used in the genetic algorithm.

| Parameter | value |
|---|---|
| $\mu$ | 3 |
| $\lambda$ | 2 |
| $\rho$ | 2 |
| $P$ | 500 |
| $Q$ | 250 |
| Probability of crossover | 0.9 |
| Probability of mutation | 0.1 |
| Maximum number of iterations | 1000 |
| Termination parameter (outer problem) | $10^{-8}$ |

## 3. Results

This section is divided in two parts. First, training sets comprising between one and ten simulated routes are fed into the proposed algorithm. These routes are composed by segments with random slopes and also randomly generated commercial velocities. The Davis model is assumed for the running resistance. Given the BSFC map and the maximum torque curve of the engine, the true velocity profiles and consumption are obtained for each of the simulated routes. The set of theoretical consumptions and the commercial speeds for each route form the training set. The estimations of the running resistance will be compared to the theoretical values for training sets of different sizes. It must be pointed out that the true velocity profiles are not fed into the algorithm, because the main purpose of the proposed method is to estimate the running resistance without GPS or VCU data.

In the second part of this section, the same algorithm has been applied to actual data measured from a diesel S2600 DHMU that operates in the north of Spain. The estimation of the average running resistance is compared to the results of a coasting test on a railway line with similar properties to those of the commercial route. Finally, the sensitivity of the proposed algorithm to the control characteristics of different drivers is studied in Section 3.2.1.

The algorithm has been implemented in Python. The parameters of the algorithm for all the experiments are collected in Table 1.

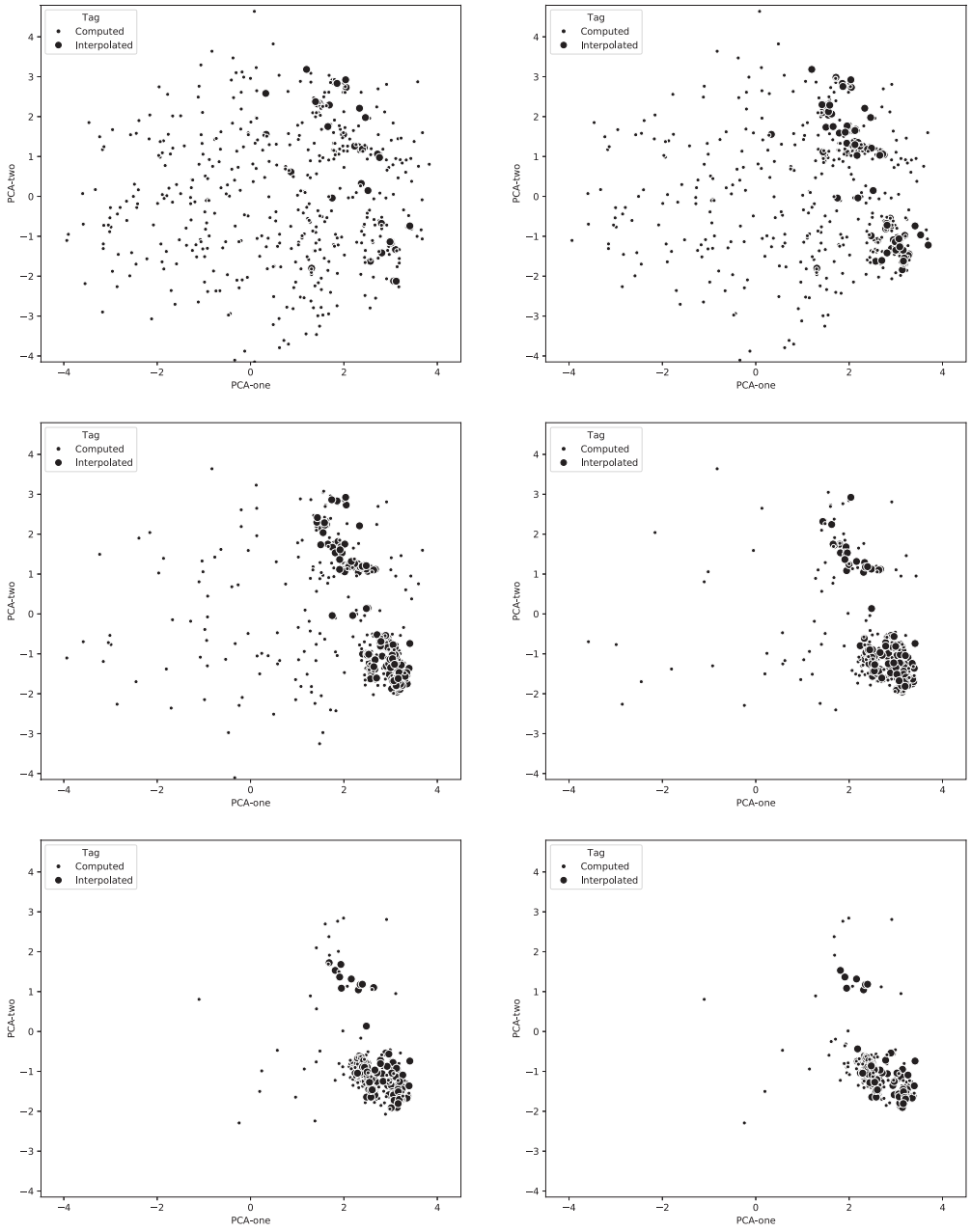


**Fig. 4.** Evolution of the BLEAQ-II population. From left to right, upper to lower: generation 100, 200, 400, 600, 800 and 1000. Larger circles are individuals where the inner problem was interpolated. Smaller circles are individuals where the inner problem was solved.

### *3.1. Simulated routes*

Routes depicted in Fig. 3 were used. Each training set is comprised of an ordered subset of these routes: subset #1 consists in the first route, subset #2 comprises the first and the second routes, etc. All routes are 3000 m long and the maximum speed is 15 m/s. Each route has a single stop. The maximum gradient (not shown) is 6 ‰. Acceleration and deceleration are limited to 0.5 m/s$^2$.

In Fig. 4, the evolution of the BLEAQ-II population is depicted. The scatter plots are Principal Component Analysis (PCA) projections of the coefficients of the running resistance (outer problem) for each individual in the population. At the initial generations, most of the individuals are tagged with the number **1** and the distribution of the individuals is uniform in the problem space. The number of individuals where the inner problem was interpolated stabilises in $Q = P/2$, and the population concentrates around the two principal local solutions of the problem. Observe that most of the interpolated individuals are near the local minima, because the density of the solutions is higher there and in step 3.b of the algorithm we have introduced a condition that prevents the interpolation of running resistances that are too far away.

Table 2 shows the theoretical consumptions of the 10 routes, and the consumptions that BLEAQ-II finds for each of the routes according to the optimised running resistance. Test results are in italics. Observe that the running resistance found if the algorithm is fed with a single route fits the consumptions of routes 2 to 9 well. Increasing the size of the training set does not produce significant gains with this metric (the accuracy is better than $10^{-3}$ for all training and test results) but these gains are clearly perceived if the expressions of the resulting running resistances are compared. In Fig. 5 the theoretical running resistance is plotted, together with its approximations taken from the consumptions

**Table 2**
Theoretical consumption on each route and BLEAQ-II predictions for datasets comprising 1, 2, 3, 5 and 10 routes. Bold numbers are the theoretical values. The consumption on routes that are not part of the training set are emphasised.

| Route | Theoretical consumption | Training Size 1 | Training Size 2 | Training Size 3 | Training Size 5 | Training Size 10 |
|---|---|---|---|---|---|---|
| 1 | **0.7012** | 0.7011 | 0.7012 | 0.7046 | 0.7012 | 0.7012 |
| 2 | **0.8915** | *0.8913* | 0.8666 | 0.8914 | 0.8915 | 0.8915 |
| 3 | **0.9412** | *0.9413* | *0.9173* | 0.9413 | 0.9413 | 0.9414 |
| 4 | **0.7083** | *0.7083* | *0.6814* | *0.7045* | 0.7083 | 0.7082 |
| 5 | **0.6310** | *0.6310* | *0.6264* | *0.6397* | 0.6310 | 0.6309 |
| 6 | **0.7033** | *0.7033* | *0.6898* | *0.7045* | *0.7033* | 0.7034 |
| 7 | **0.9486** | *0.9490* | *0.9120* | *0.9469* | *0.9486* | 0.9504 |
| 8 | **0.7047** | *0.7047* | *0.6867* | *0.7082* | *0.7047* | 0.7046 |
| 9 | **0.9106** | *0.9099* | *0.8896* | *0.9116* | *0.9106* | 0.9093 |
| 10 | **0.5989** | *0.5988* | *0.5981* | *0.6022* | *0.5989* | 0.5987 |

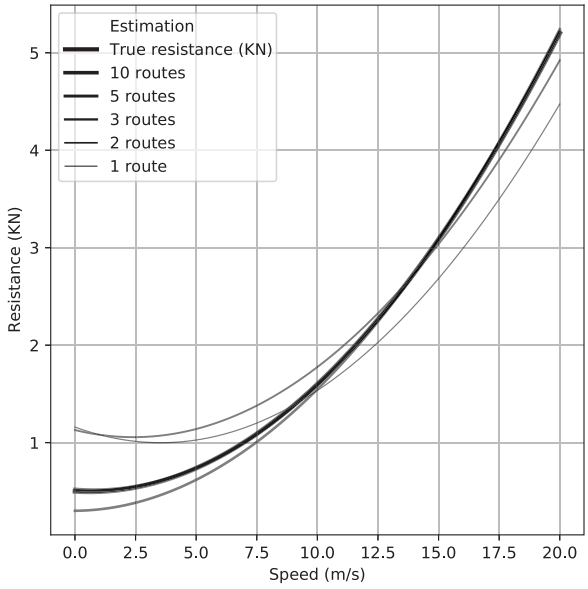


**Fig. 5.** Theoretical running resistance and BLEAQ-II approximations from datasets comprising 1, 2, 3, 5 and 10 routes. Approximations from 5 and 10 routes are almost identical to the true resistance.

on 1, 2, 3, 5 and 10 routes. The solutions for 5 and 10 routes are indistinguishable from the theoretical curve.

### 3.2. Field experiments

The presented algorithm has been applied to real data measured from a S2600 DHMU that operates on a 94 Km long route in the north of Spain (47 Kms of rail, outward and return). The maximum commercial speed is 14 m/s and the maximum gradient on the route is 16 ‰. The reported average consumption for the vehicles that operate on that route is 82 litres of fuel every 100 km.

The test section is an unused branch of the same commercial line, with a length of 3400 m. The maximum gradient of this section is 13 ‰. The test vehicle is a RENFE S2600 railcar with hydrodynamic-mechanical transmission and a laden mass of 54,000 kg. The speed profile of the tests is shown on the left side of Fig. 6. The speed sampling period is 1 s. Traction was disconnected between kilometre points 0.9 and 2.2 in the outbound direction, and between kilometre points 1.4 and 0.9 in the return direction. In the right part of the same figure a detail of the speeds sampled between kilometre points 1 and 1.2 in both directions is shown. To compensate for the gradient effects, straight lines were fitted to outbound and return paths by linear regression. The slope of the regression line in the outbound section is 0.070 m/s$^2$, and in the return section it is 0.083 m/s$^2$, so it is estimated that the mean deceleration of the vehicle in a straight and horizontal section is 0.076 m/s$^2$, which corresponds to a running resistance of 4.10 KN at 12 m/s.

The BLEAQ-II estimated running resistance for the aforementioned 94 km commercial route and a consumption of 82 l every 100 km is $4193.6 + 4.6 \cdot v + 0.054 \cdot v^2$, which is 4.26KN at 12 m/s. The parameters of the genetic algorithm are the same as those indicated in Section 3.1.

In Fig. 7 different estimations of the running resistance at 12 m/s have been plotted on a graph against hypothetical consumptions between 70 and 100 l, illustrating the interdependence between the estimated resistance and the measured consumption. The measured resistance is represented by a horizontal dotted line and the genetic estimation for 82 litres is marked with a dashed line. Box plots measure the sensitivity of the algorithm to the driving styles of different drivers, as discussed below.

#### 3.2.1. Changes in fuel consumption related to the driver's driving style

In the driving of a railcar the main control element is a joystick with which the speed of the vehicle is set. Legally regulated acceleration and braking limits are in place, and on the track there are different indications about the maximum speeds of the section and the points at which the manoeuvre must be started so that the maximum speed established for each section is not exceeded. According to Martinez-Garcia et al. (2019), drivers react to visual stimuli after a certain time delay (199 ms on average for joystick control) so it is reasonable to assume the variability in reaction times will introduce uncertainty in the model output. Along the same lines as in the reference (Šíra et al., 2020), in this section we propose a sensitivity study to estimate the variations in energy estimation for different driving styles.

The basic driving strategy consists of keeping the vehicle at the nominal speed for as long as possible, accelerating and decelerating in well-defined positions, as mentioned above. To approximate the effect of far-point error in human-centred driver models (Martinez-Garcia and Gordon, 2018), we have studied the effect of delaying or bringing forward the points at which the driver initiates the acceleration and braking manoeuvres. In any case, we continue to use the code that ensures that the vehicle does not exceed the speed limits, that excessive torque is not demanded from the engine and that the train stops at all stations.

Fifty simulations of the model have been carried out for running resistance values between 500 and 8000 N and maximum accelerations between 0.25 and 0.75 m/s$^2$, reflecting the different driving styles. In cases where the simulation leads to travel times longer than the target value, the times at each stop are reduced proportionally to their duration, and vice versa. The results are shown in Fig. 7. Note that the dispersion decreases with running resistance, and is higher at some particular values, such as 71 l/h. These values are related to the hydraulic to mechanical gearbox shift modes. From this study we can conclude that the magnitude of the uncertainty introduced in the model due to the driver's action is less than 2% in the range of consumption handled.

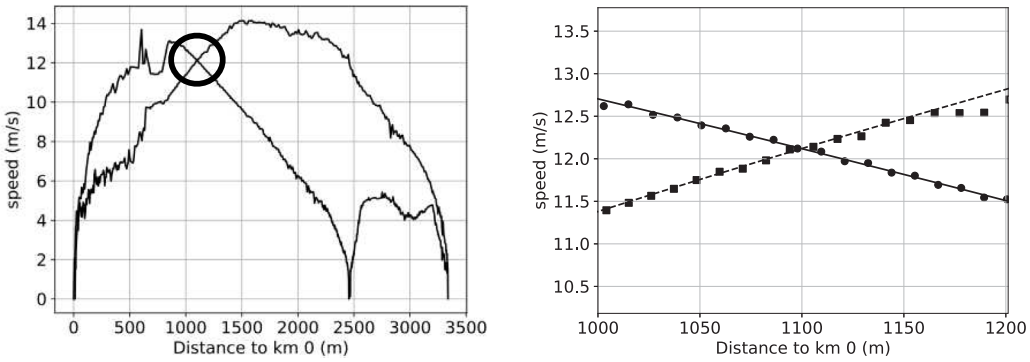


**Fig. 6.** Left: Speed profile of the test section. The circle marks the point where the vehicle was not tractioning. Right: Detail of the speed samples at the non-tractioning point and linear models fitted to the speed values. Squares: outbound direction. Circles: inbound direction. The average deceleration for speeds between 11 and 13 m/s is 0.076 m/s$^2$.

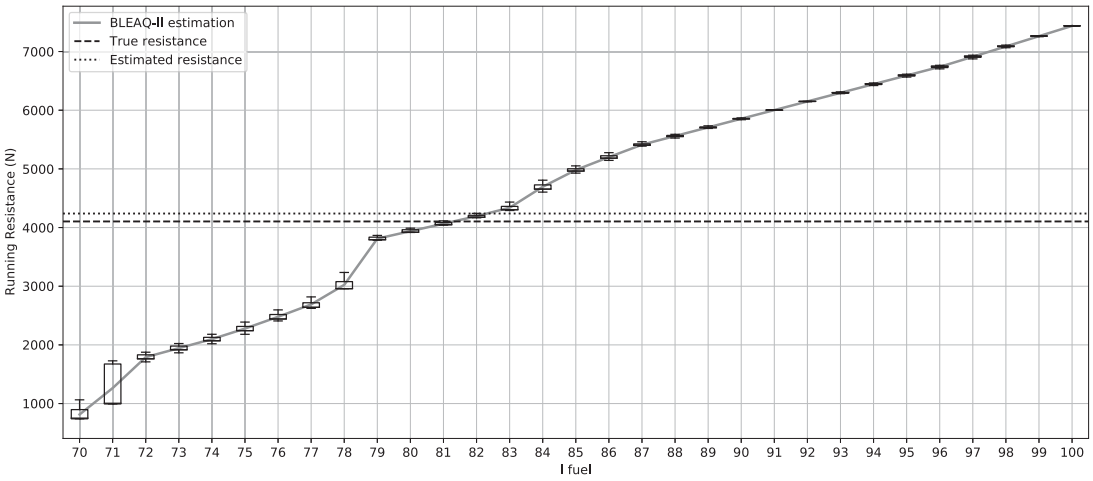


**Fig. 7.** Estimated running resistances for fuel consumptions between 70 and 105 litres every 100 km. The coasting test thew a result of 4.10KN (dashed line), which is in good agreement with the 4.26KN estimated with the genetic algorithm (dotted line) for 82 litres. The box plots show the dispersion of the results for different control strategies in driving. Dispersion decreases with forward resistance, and is higher at some particular values, such as 71 l/h, related to the hydraulic to mechanical gearbox shift modes.

## 4. Concluding remarks and future work

We have shown that the approximation of the running resistance from operation data is feasible when the average consumption of the train is known for a small set of routes. This kind of approximation is coherent from a theoretical point of view, as shown in Section 3.1, however it is only moderately accurate in practice, as seen in the field tests. In any case, it is helpful for indirectly estimating consumption and emissions on new routes or, as suggested in this paper, for evaluating the impact of alterations in the vehicle such as the transformation from Diesel to GNL that originated this study. The main advantage of the proposed procedure lies in its cost: this is a purely numerical algorithm that operates with data that is readily available, not requiring additional acquisition of equipment or test drives.

From a methodological point of view, it has also been shown that the optimisation of the coefficients of the Davis model from long-term consumption data is an ill-conditioned problem, with multiple local minima and heavy computational requirements. Recently developed bilevel evolutionary algorithms were successfully deployed to solve this task. It is important to make clear that the methodology that has been proposed is not limited to quadratic models of the running resistance. In future studies, different machine learning-based models, such as neural networks or rule-based models, could be deployed to obtain more realistic expressions of the running resistance. Likewise, the model can also be completed by introducing parameters describing the characteristics of the driver, following Martinez-Garcia and Gordon (2018) and Martinez-Garcia et al. (2019).

## CRediT authorship contribution statement

**Luciano Sánchez:** Conceptualization, Methodology, Software, Writing – review & editing, Supervision. **Pablo Luque:** Conceptualization, Methodology, Investigation, Writing – review & editing. **Daniel Álvarez:** Conceptualization, Methodology, Investigation, Writing – review & editing.

## Declaration of competing interest

The authors declare that they have no known competing financial interests or personal relationships that could have appeared to influence the work reported in this paper.

## Acknowledgements

This work has been partially supported by the Ministry of Economy, Industry and Competitiveness (“Ministerio de Economía, Industria y Competitividad”) from Spain/FEDER under grants TIN2017-84804-R and PID2020-112726RB-I00 and by the Regional Ministry of the Principality of Asturias (“Consejería de Empleo, Industria y Turismo del Principado de Asturias”), Spain under grant GRUPIN18-226.

## References

Besinovic, N., Quaglietta, E., Goverde, R.M., 2013. A simulation-based optimization approach for the calibration of dynamic train speed profiles. J. Rail Transp. Plan. Manag 3 (4), 126–136.

Boggs, P.T., Tolle, J.W., 1995. Sequential quadratic programming. Acta Numer. 4 (1), 1–51.

Davis, W.J., 1926. The Tractive Resistance of Electric Locomotives and Cars. General Electric.

Eaton, J., Yang, S., Gongora, M., 2017. Ant colony optimization for simulated dynamic multi-objective railway junction rescheduling. IEEE Trans. Intell. Transp. Syst. 18 (11), 2980–2992. http://dx.doi.org/10.1109/TITS.2017.2665042.

Fernández-Rodríguez, A., Su, S., Fernández-Cardador, A., Cucala, A.P., Cao, Y., 2020. A multi-objective algorithm for train driving energy reduction with multiple time targets. Eng. Optim. 1–16.

Hansen, H.S., Nawaz, M.U., Olsson, N., 2017. Using operational data to estimate the running resistance of trains. estimation of the resistance in a set of norwegian tunnels. J. Rail Transp. Plan. Manag 7 (1), 62–76. http://dx.doi.org/10.1016/j.jrtpm.2017.01.002.

He, D., Zhang, L., Guo, S., Chen, Y., Shan, S., Jian, H., 2021. Energy-efficient train trajectory optimization based on improved differential evolution algorithm and multi-particle model. J. Cleaner Prod. 304, 127163.

Huang, S.-R., Sung, H.-K., Ma, C.-H., 2015. Optimize energy of train simulation with track slope data. In: 2015 IEEE 18th International Conference on Intelligent Transportation Systems. pp. 590–597. http://dx.doi.org/10.1109/ITSC.2015.103.

Huang, Y., Yang, L., Tang, T., Gao, Z., Cao, F., 2017. Joint train scheduling optimization with service quality and energy efficiency in urban rail transit networks. Energy 138, 1124–1147.

Kikuchi, S., 1991. A simulation model of train travel on a rail transit line. J. Adv. Transp. 25 (2), 211–224.

Martínez Fernández, P., Villalba Sanchís, I., Yepes, V., Insa Franco, R., 2019. A review of modelling and optimisation methods applied to railways energy consumption. J. Cleaner Prod. 222, 153–162.

Martinez-Garcia, M., Gordon, T., 2018. A new model of human steering using far-point error perception and multiplicative control. In: 2018 IEEE International Conference on Systems, Man, and Cybernetics (SMC). pp. 1245–1250. http://dx.doi.org/10.1109/SMC.2018.00218.

Martinez-Garcia, M., Zhang, Y., Gordon, T., 2019. Memory pattern identification for feedback tracking control in human–machine systems. Human Factors 0018720819881008.

Nino-Ruiz, E.D., 2021. Editorial: Special issue of IJAI on machine learning methods for inverse problems. Int. J. Artif. Intell. 19 (1), 77–79.

Pan, Y., Chen, S., Qiao, F., Ukkusuri, S.V., Tang, K., 2019. Estimation of real-driving emissions for buses fueled with liquefied natural gas based on gradient boosted regression trees. Sci. Total Environ. 660, 741–750. http://dx.doi.org/10.1016/j.scitotenv.2019.01.054.

Peralta, D., Bergmeir, C., Krone, M., Galende, M., Menéndez, M., Sainz-Palmero, G.I., Martinez Bertrand, C., Klawonn, F., Benitez, J.M., 2018. Multiobjective optimization for railway maintenance plans. J. Comput. Civ. Eng. 32 (3).

Pineda-Jaramillo, J., Martínez-Fernández, P., Villalba-Sanchis, I., Salvador-Zuriaga, P., Insa-Franco, R., 2020. Predicting the traction power of metropolitan railway lines using different machine learning models. Int. J. Rail Transp 1–18.

Rochard, B.P., Schmid, F., 2000. A review of methods to measure and calculate train resistances. Proc. Inst. Mech. Eng. F: Journal of Rail and Rapid Transit 214 (4), 185–199. http://dx.doi.org/10.1243/0954409001531306.

ShangGuan, W., Yan, X.-H., Cai, B.-G., Wang, J., 2015. Multiobjective optimization for train speed trajectory in CTCS high-speed railway with hybrid evolutionary algorithm. IEEE Trans. Intell. Transp. Syst. 16 (4), 2215–2225.

Sicre, C., Cucala, A., Fernández-Cardador, A., 2014. Real time regulation of efficient driving of high speed trains based on a genetic algorithm and a fuzzy model of manual driving. Eng. Appl. Artif. Intell. 29, 79–92.

Sinha, A., Lu, Z., Deb, K., Malo, P., 2020. Bilevel optimization based on iterative approximation of multiple mappings. J. Heuristics 26 (2), 151–185.

Šíra, M., Cucala, A.P., Fernández-Cardador, A., Fernández-Rodríguez, A., 2020. Sensitivities and uncertainties of eco-driving algorithm estimating train power consumption. In: 2020 Conference on Precision Electromagnetic Measurements (CPEM). IEEE, pp. 1–2.

Somaschini, C., Rocchi, D., Tomasini, G., Schito, P., 2016. Simplified estimation of train resistance parameters: Full scale experimental tests and analysis. In: Proceedings of the Third International Conference on Railway Technology: Research, Development and Maintenance.

Su, S., Tang, T., Li, X., 2018. Driving strategy optimization for trains in subway systems. Proc. Inst. Mech. Eng. F: J. Rail and Rapid Transit 232 (2), 369–383.

Suarez-Bertoa, R., Pechout, M., Vojtisek, M., Astorga, C., 2020. Regulated and non-regulated emissions from euro 6 diesel, gasoline and CNG vehicles under real-world driving conditions. Atmosphere 11 (2), 204. http://dx.doi.org/10.3390/atmos11020204, URL: http://dx.doi.org/10.3390/atmos11020204.

Tang, H., Wang, Y., Liu, X., Feng, X., 2020. Reinforcement learning approach for optimal control of multiple electric locomotives in a heavy-haul freight train: A double-switch-Q-network architecture. Knowl.-Based Syst. 190, 105173.

Tarantola, A., 2005. Inverse Problem Theory and Methods for Model Parameter Estimation. SIAM.

Tormos, B., Martín, J., Pla, B., Jiménez-Reyes, A.J., 2020. A methodology to estimate mechanical losses and its distribution during a real driving cycle. Tribol. Int. 145, 106208. http://dx.doi.org/10.1016/j.triboint.2020.106208.

Vicente, L., Savard, G., Júdice, J., 1994. Descent approaches for quadratic bilevel programming. J. Optim. Theory Appl. 81 (2), 379–399.

Wang, J., Rakha, H.A., 2018. Longitudinal train dynamics model for a rail transit simulation system. Transp. Res. C 86, 111–123.

Wu, Q., Spiryagin, M., Cole, C., 2016. Longitudinal train dynamics: an overview. Veh. Syst. Dyn 54 (12), 1688–1714.

Yang, H., Liu, H., Fu, Y., 2015. Multi-objective operation optimization for electric multiple unit-based on speed restriction mutation. Neurocomputing 169, 383–391, Learning for Visual Semantic Understanding in Big Data ESANN 2014 Industrial Data Processing and Analysis.

Yu, C., Seslija, M., Brownbridge, G., Mosbach, S., Kraft, M., Parsi, M., Davis, M., Page, V., Bhave, A., 2020. Deep kernel learning approach to engine emissions modeling. Data-Centric Eng 1, e4. http://dx.doi.org/10.1017/dce.2020.4.